A simplified 3D urban unit representation for urban microclimate simulations: A case study in China's 'Hot Summer and Cold Winter' climate zone.

Leonidas BOURIKAS[1], Patrick A.B. JAMES[1], AbuBakr S. BAHAJ[1], Mark F. JENTSCH[2], Tianfeng SHEN[3], David H.C. CHOW[4], Jo DARKWA[5],

[1] *Energy & Climate Change Division, Sustainable Energy Research Group (SERG), Faculty of Engineering and the Environment, University of Southampton, Southampton SO17 1BJ, UK*
[2] *Urban Energy Systems, Bauhaus-Universität Weimar, Weimar, Germany*
[3] *Centre for Sustainable Energy Technologies (CSET), University of Nottingham Ningbo, P.R. China*
[4] *School of Architecture, Faculty of Humanities and Social Sciences, University of Liverpool, UK*
[5] *Faculty of Engineering, University of Nottingham, UK*

Abstract: Urban and building energy simulations are usually initiated with typical meteorological year weather data. However, the locations where these historical datasets were collected (usually airports) do not represent the local, site specific micro-climates that cities develop. An idealised "urban unit model" (250m radius) has been developed for use with simulation modelling as a method for adapting commonly available weather data files to the local micro-climate. The idealised "urban unit model" presented in this work is based on the main thermal and morphological characteristics of nine sites with residential / institutional (university) use in Hangzhou, China. This newly introduced idealised "urban unit model" was implemented into micro-climatic simulations using a Computational Fluid Dynamics – Surface Energy Balance analysis tool (ENVI-met, Version 4). Following model validation, two scenarios were developed, one for assessing the impact of vegetated surface's location on air temperature in relation to the air temperature measurement point (3.5m above ground) and a second one for analysing the effect of the vegetated surface area on the average urban unit (250m radius) air and surface temperature. The performance of the "urban unit model" was deemed satisfactory and the performance evaluation indices were comparable to previously published work (RMSE:1.3; MAPE:3.1%).

The results of Scenario 1 (spatial distribution of green space in the urban unit) showed that the location of the vegetated surface had only marginal impact on the air temperature at the middle grid cell of the urban unit. As would be expected, the air temperature was lower for the case where the vegetation was at the centre of the model. Scenario 2 (changing the green space percentage in the urban unit) revealed that the increase of green space resulted in an increase in the occurrence frequency of air temperatures towards the cooler end of the temperature distribution. This study concluded that in places with a humid subtropical climate such as Hangzhou, for successive hot, dry summer days, the reduction in soil water content can negate, to a large extent, the cooling benefits of added vegetation. This work presents a methodology that addresses the implications of urban morphology representation for micro-climate modelling.

Keywords: idealised urban model, micro-climate simulations, vegetation, urban air temperature, cities

1. INTRODUCTION

Urban and building energy simulation models are usually initiated with hourly weather datasets for a 'typical' year (8,760 hours) (Crawley, 1998: page 1). Common typical weather year formats have the form of a synthetic year with months representative of the climatic conditions for the site of interest (Hacker et al., 2009: page 4). One important consideration for the use of these typical year weather time series in energy simulations is the representativeness of the location where the source data were collected. Many of these locations are at airports nearby large cities. However, locations within the city develop local, site specific micro-climates that cannot always be represented by these historical datasets (Mylona, 2012: page 59). This work aims to provide a more comprehensive methodology that delivers a more appropriate and relevant analysis of urban micro-climates.

This paper introduces an idealised "urban unit model" (on a 250m radius) that represents the main thermal and morphological characteristics of urban sites at the neighbourhood scale. This model can be used with simulations as a method for adapting commonly available weather data files to the local micro-climate. A case study was developed for the assessment of (1) the impact of vegetated surface's location on air temperature in relation to the air temperature measurement point (3.5m above ground) and (2) the effect of the vegetated surface area on the average urban unit (250m radius) air and surface temperature in places with a humid subtropical climate such as the case study city Hangzhou, China.

2. METHODOLOGY

A small size neighbourhood was selected as the scale of interest. Therefore, the size of an "urban unit" has been defined as a disk with a radius of 250m around a temperature and relative humidity sensor with a data logger. Air temperature and relative humidity were collected at 26 urban sites in Hangzhou (30˚15'N 120˚10'E) in Zhejiang Province, China (Bourikas et al., 2013: page 8; Shen et al., 2014: page 4). The sensors were installed on lampposts at a level 3m to 5m above ground. They measured and logged air temperature at 11-Bit (0.0625˚C) resolution and relative humidity at 12-Bit (0.04%) resolution (Maxim Integrated, 2013). The manufacturer stated air temperature accuracy is +/-0.5 °C and the RH accuracy is +/- 5% (Maxim Integrated, 2013). For calibration purposes air temperature (°C) and RH (%) readings within 1 minute intervals were compared to the readings of two separate thermocouples in an environmental chamber at ambient air temperatures of -10 °C, 0 °C, 10 °C and 40 °C (Shen et al., 2013: page 4). The results showed that all the sensors operated within the reported accuracy margin and fitted well to the thermocouple measurements (Shen et al., 2013: page 4).

Air temperature and relative humidity observations in the surface layer can be expected to be representative of an area ranging from 100m to several hundred meters in a direction upwind and around each sensor (Oke, 2006: page 8). However, most of the sensors were collecting measurements in the roughness sub-layer and not in the surface layer (Cheng & Castro, 2002: page 231) (Figure 1). The location of the measurement sites was carefully selected to have as homogeneous characteristics as possible for a large city and the sensors were installed with a reasonable distance to points of noticeable surface type change (Bourikas et al., 2013: page 8).

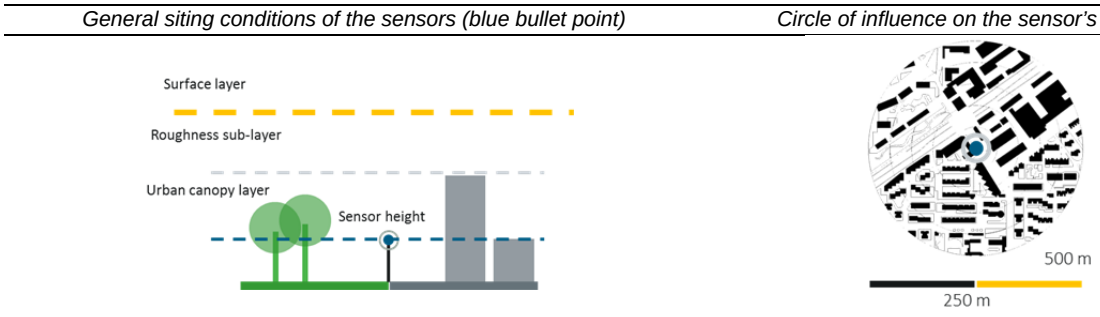

Figure 1: Siting of selected sensors in Hangzhou and representation of the size of the" urban unit" (Top Right).

The impact of the urban unit's size was analysed by assessing the vegetation cover's influence on air temperature. Twelve urban sites were selected across the city centre in Hangzhou (Northern part above Qiantang River, Figure 2) in order to examine the urban unit borders' extent. Each sensor was considered to be the centre of concentric circles at radii of 10m, 25m, 50 m, 100m, 150m, 200m, 300m, 400m and 500m. Then the footprint of the vegetated surface was estimated and apportioned to these annuli areas (Figure 3).

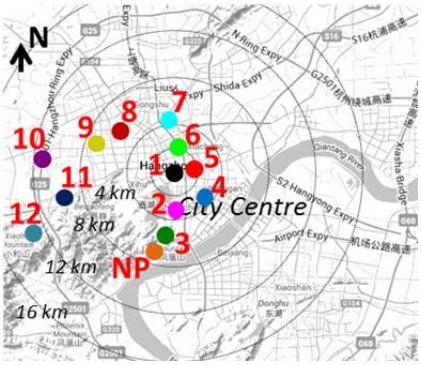

Figure 2: Location of the12 sites for the urban unit size assessment (Left) and a typical fisheye image used for estimating the Sky View Factor in Hangzhou (Right). (Note: The colour scheme of the bullet points in the map is consistent with Figure 3.)

The analysis was carried out for 14 weeks of hourly data collected during summer 2013. The air temperature (T_{air}) shown in Figure 3 is the mean air temperature departure from the mean temperature of the twelve sensors in this group. The vertical shaded reference line marks the 250 m radius from the centre (sensor). The legend shows the mean summer air temperature departure from the group's mean and the goodness of fit of the non-linear regression line in parentheses (Figure 3).

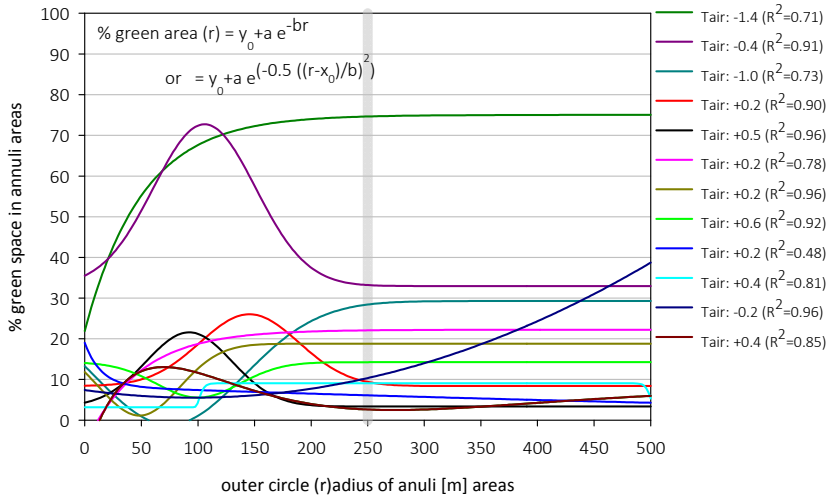

Figure 3: Regression lines of the percentage vegetated area in each annulus area on the distance from the centre (sensor).

It would be expected that the influence of green space is larger when closer to the sensor and diminishes if it is more towards to the outer annuli areas. The strong influence of vegetated areas is evident from the first peak of vegetated surface area in comparison to the general trend in the group of sensors. The locations of sensors 3 (dark green; -1.4 °C) and 10 (purple; -0.4 °C) have a lower than the group average air temperature and their vegetated surface area is large with an early peak within the first 100 meters from the sensor (Figure 3). Interestingly, sensor 12 (dark cyan; -1.0 °C) which also shows a negative temperature departure from the group mean has a small vegetated area in the first 150 meters away from the sensor, comparable with those at locations with higher than the group average temperature. Its negative trend seems to be explained with the steep rise in vegetated surface area at the annuli area from 150 to 200 meters, showing that the influence of vegetation remains strong at this distance (Figure 3). Further evidence comes from the comparison between sensor 1 (black, +0.5 °C) and sensors 2, 5 and 9 (pink, red, gold; +0.2 °C). The regression trend lines indicate that the location where sensor 1 resides is warmer than the locations of sensors 2, 5 and 9 despite the larger vegetated surface within a 0 to 100m radial distance from the sensor. In the case of sensors 2, 5 and 9 the vegetated surface area peaks occur later at distances from 100 to 150 meters showing the persistent impact of the green space area. In addition, site 5 (red; +0.2 °C) has a similar vegetated surface area to site 1 (black; +0.5 °C) with the only difference being a delay of the peak, that is seen at distances 50 to 100 m farther outwards. Sensor 11 (dark blue, -0.2 °C) has a lower air temperature than the group average but the green space percentage peak occurs after

the 250m radius border. However, in this case the low air temperature is mainly attributed to the site's proximity to a large wetland (i.e. Xixi). Based on these results a conservative estimate is therefore made for a representative circular "urban unit" with a 250m radius. It is expected that the total area of 196,350m^2 (250m radius) surrounding the sensor will be the representative part of the source area for the air temperature and relative humidity signal. The size of the proposed urban unit agrees with other authors' studies for the sufficient windward distance from a point of roughness or thermal change (~200-500m) and the internal boundary layer extent in zones within local climate classification schemes (r ~ 200-500m) (Stewart & Oke, 2012: page 1889).

2.1. Land cover analysis and urban classification

This study adopts a combination between a local urban classification scheme and the simulation of the local specific weather development for urban unit layouts with a typical residential / institutional (university, college) use in the case study region. Micro climatic simulation modelling is used to assess the influence of the pervious surface ratio (P_r) on the local, street level air temperature. The main advantage of using a surface classification scheme is that it provides generic input data for the simulation modelling (Stewart & Oke, 2012: 1893) and the simulation results can be attributed back to typical urban morphology characteristics.

A visual inspection of aerial and eye view images was considered to suit well to the scale and scope of the analysis. Step 1 - Each sensor was set at the centre of a circular area (i.e. disk) of a 250m radius (Figure 4). Step 2 - A selection of metadata (e.g high resolution images taken on site) was used to draw polygons for the vegetation (green colour), water (blue colour) and buildings' (black colour) surfaces (Figure 4). The residual was designated as other impermeable surface (white colour) and it included street and pavement surfaces. A set of morphological parameters was then calculated for each site including: the mean building height $\overline{H}$, the roughness length z_0, the height to width aspect ratio, the frontal area ratio λ_f, the building surface fraction F_r, the impervious surface fraction I_r and the pervious surface fraction P_r.

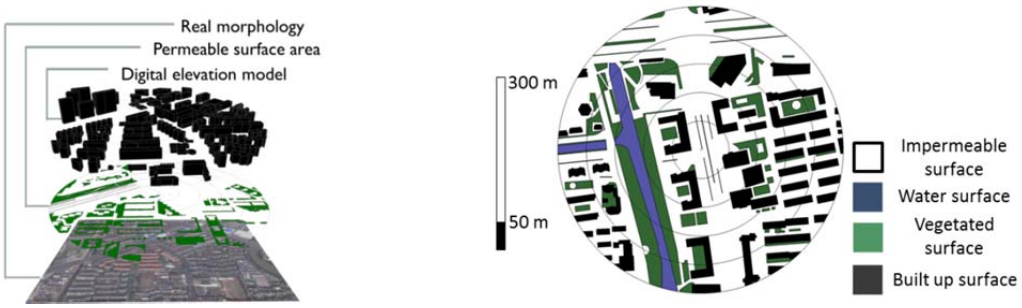

Figure 4: The digital elevation model and the land cover are built based on the metadata (Left). Four land surface types have been identified and their surface area is estimated by the model. The sensor is located at the centre of a disk of 250m radius (Right).

Each urban unit was classified according to the land cover analysis into a "Local Climate Zone" following an urban classification scheme developed by Stewart and Oke (2012). Each zone (i.e. thermally homogenous regions of uniform surface characteristics) in the scheme exhibits a distinctive diurnal temperature development profile at "screen" height (~1.5 to 3m) at the local scale (Stewart & Oke, 2012: page 1884). The resulting Local Climate Zones (LCZs) describe 17 generic environments consisting of 10 zones for built (e.g. open high-rise) and 7 for non-urban land cover types (e.g. scattered trees) (Stewart & Oke, 2012: page 1886). Each zone is represented by a set of ten morphological parameters and a descriptive definition of the typical location and use of the urban sites classified into a zone.

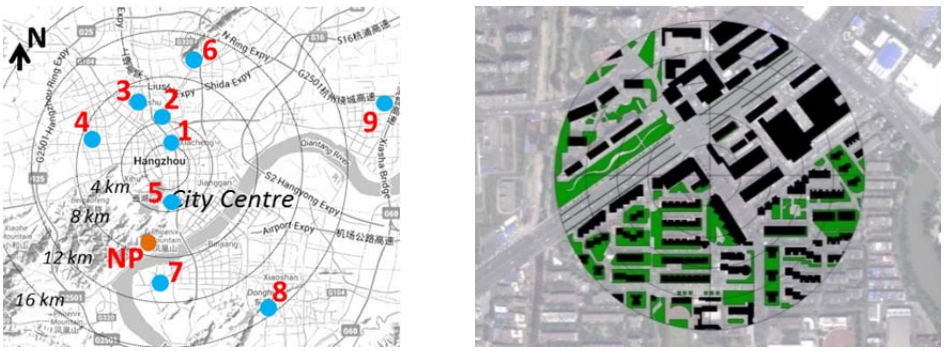

Figure 5: The nine studied urban units classified into LCZ 5 (locations, marked with blue bullets) in Hangzhou (Left).(Note: The Mantou Mountain, National Principle Weather station's location (reference, typical meteorological year file source) is marked as NP). Example of the land cover analysis for Site 2 (Right). Buildings are marked with black and vegetation with green.

Nine urban units out of a total of 26 investigated areas in Hangzhou were classified as "Local Climate Zone 5" (LCZ5) (Figure 5). Three additional sites were removed from the study because of their proximity to large water bodies and large inhomogeneities in their surface characteristics. This study will focus on the nine sites classified as "LCZ5".

2.2. A simplified model for urban micro-climatic simulations

In idealised models building geometry is usually substituted with arrays of cubes. Typical methods use cubes in staggered or aligned arrays (e.g. Cheng & Castro, 2002; Xie & Castro, 2006; Santiago et al., 2007; Kanda & Moriizumi, 2009; Millward-Hopkins et al., 2013). Cubes in regular arrays are spaced in repeated intervals equal at all directions to the cube's edge length (i.e. aspect ratio = 1) (Figure 6).

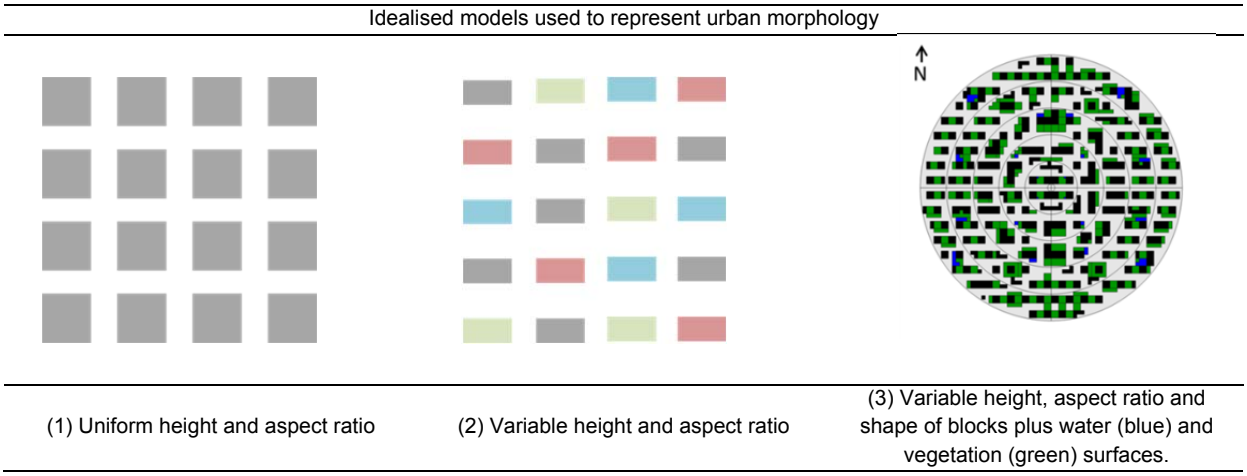

Figure 6: Typical urban morphology representations with idealised models (Left & middle) and the idealised "urban unit model" in this study (Right). (1) and (2) in figure were adapted from Millward-Hopkins et al. (2013) page: 449.

In this study, the generic "urban unit model" comprises of square based boxes (i.e. blocks) with a non-uniform height in a staggered irregular array (Figure 6, right). The staggered block array has a North-South orientation. Each block has a base of 3m x 3m (9 m^2). Blocks can be combined on the horizontal (not in height) at any possible number and shape. Each block can represent a building (black), vegetated surface (green, grass or tree) or water surface (blue, zero height). The residual space between the blocks represents the impervious surface (grey, e.g. roads, paved) (Figure 6, right). The generic, idealised "urban unit model" has a similar planar area ratio and mean weighted (footprint) building height to the nine studied sites. The individual surface energy balances are represented in the model by the pervious, impervious and building footprint surface area ratios. The centre of the urban unit is always surrounded by an "empty" disk with a periphery at a radius equal to the computational grid resolution. Empty means that the surface of the central disk can either be pervious surface (e.g. vegetation) or impervious surface (e.g. road) but not a building.

Table 1: Overview of the median and the (range) for 80% of the key morphological parameter observations from the nine investigated sites. (R-r refers to the inner and outer radius of the annuli borders)

Annulus R-r (m)	$\overline{H}$ (m)	P_r (%)	I_r (%)	λ_f(%)	F_r(%)	d (m)	z_0 (m)
0-50	20	7	72	17	21	6.7	1.8 (1.3-4)
	(15–22)	(0-15)	(50-85)	(7-25)	(7-30)	(3.6-11.1)	
50-100	18	11	61	15	27	8.9	1.4 (0.5-3)
	(13-25)	(0-17)	(54-70)	(6-20)	(8-40)	(3.6-12.9)	
100-150	20	15	65	13	23	7.6	1.8 (0.5-3)
	(13-24)	(0-25)	(56-70)	(6-20)	(4-30)	(2.0-10.6)	
150-200	17	15	60	14	24	8.6	1.2 (0.7-2)
	(12-20)	(5-25)	(50-66)	(10-17)	(19-28)	(5.5-9.7)	
200-250	19	15	56	13	23	8.3	1.8 (0.7-3)
	(16-24)	(12-25)	(54-66)	(10-20)	(16-27)	(5.8-11.3)	

The morphology characteristics of each annulus area were based on the median value observations from the statistical analysis for the nine LCZ5 urban units (Table 1). The median was preferred over the mean because it is not affected by extremely low or high values and the calculated distributions were rather skewed than normal. The pervious surface area ratios increase with the increase of the distance from the centre of the urban unit (Table 1). This positive correlation (Spearman's $r_s(43)=0.503 > 0.294$ ($p=0.05$)) is specific to Hangzhou but it is meaningful for the wider study of temperature development in relation to green space in the context of Hangzhou. The distance between the blocks in each annulus area is random and the number of blocks was defined by the F_r ratio

observations. The distribution of the blocks in each annulus area is similar in all notional quarter annuli. The changes to the packing density and distance between the blocks had produced a randomly dispersed layout that is expected to fit better to the high spatial inhomogeneity of real cities than a regular staggered cube array.

3. URBAN MORPHOLOGY SCENARIOS

Two scenarios have been investigated for assessing the sensitivity of the model to the area covered by vegetation and its impact on the air temperature development. The first scenario (Scenario 1) compared the air temperature at 3.5m height above ground ($T_{3.5m}$) in Case 1, where the vegetation was distributed according to the statistical results, with Case 2, where all the vegetation surface area was moved to the centre of the urban unit and Case 3 where the vegetated area was moved towards the outer annuli (Figure 7). The pervious surface area ratio (0.15) remained the same for the urban unit at all cases.

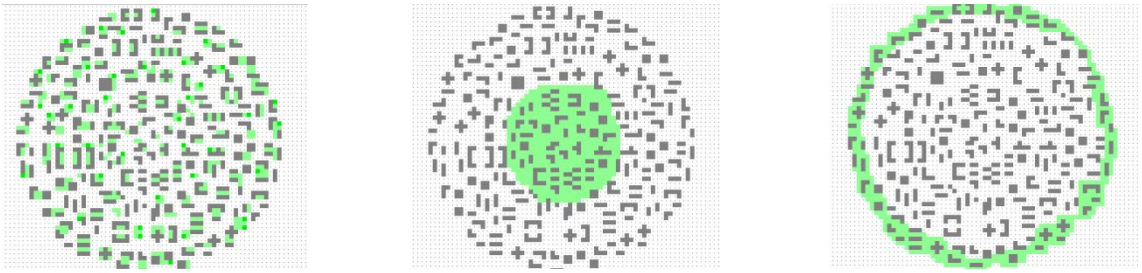

Case 1. Vegetation distribution according to annuli areas' statistics | *Case 2. Vegetated surface moved into the central annuli areas (centric)* | *Case 3. Vegetated surface moved out to the outer annuli areas (outer)*

Figure 7: Different distribution of the vegetated surface area in the urban unit for the cases considered in Scenario 1.

Scenario 2 compared the air temperature ($T_{3.5m}$) from Case 1 with 5 additional Cases (4 to 8) that had increasing ratios of pervious surface area that was distributed evenly (same percentage) in each annulus area (Figure 8). Each case had 5%-points more vegetated surface area (i.e. in the form of grass) than the previous one up to a maximum of $P_r = 0.4$ which represents the upper limit for the "Local Climate Zone 5" classification.

Scenario 2	pervious surface fraction P_r	
Case 1	15%	
Case 4	20%	
Case 5	25%	
Case 6	30%	
Case 7	35%	
Case 8	40%	*Case 4.* $P_r = 0.2$

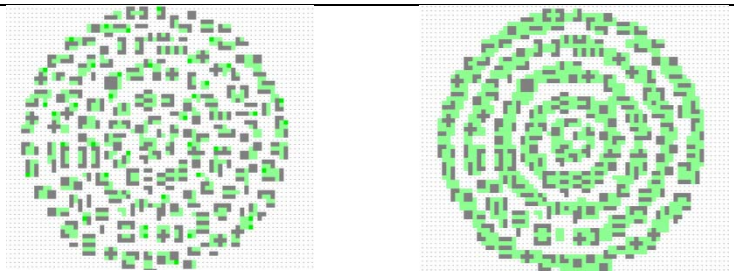

Case 8. $P_r = 0.4$

Figure 8: The different percentages of vegetated surface area in the "urban unit" for the cases in Scenario 2. Top plan view of the computational domain (Right) for the cases with $P_r = 0.2$ and $P_r = 0.4$.

The air temperature development in the idealised "urban unit" for both scenarios was simulated with ENVI-met (Version 4) for August 10, 2013 which represented a sunny hot day in Hangzhou. On the 10th of August 2013 the mean ambient temperature was 36 °C. The average RH was 44% and the wind was blowing from a South – South West direction with an average speed of about 2 m/s (The Weather Underground, 2014). The sky was clear. The previous four days had been dry with 41 °C maximum air temperature and similar weather conditions as the day of the simulations. The analysis was conducted for 24 hours from 00:00 China Standard Time (CST) to 23:00 CST. To validate the simulation results obtained with the idealised "urban unit", the average air temperature ($T_{3.5m}$) simulation results (average across all the disk area of the urban unit excluding buildings) were compared against the average air temperature observations from the nine studied sites in Hangzhou (Figure 9).

3.1. Micro-climatic simulations

ENVI-met is a three dimensional non-hydrostatic numerical micro-climate model that couples an atmospheric, a soil and a one-dimensional (1-D) vegetation model and the surface energy balance. The atmospheric model is based on the incompressible Reynolds averaged Navier Stokes (RANS) equations (Bruse & Fleer, 1998: page 374). The boundary layer is reproduced with a 1-D model that extends up to 2500 m and provides the inflow (i.e. only in the case of forced boundary conditions at the inflow) and top boundary conditions to the 3-D domain

(Bruse & Fleer, 1998: page 374). The boundary layer model is usually initiated with regional weather conditions (i.e. measured data from a nearby airport weather station). Wind speed and direction remain constant during the simulation while the effect of the surrounding urban environment can be modelled with the use of cyclic (periodic) lateral and outflow boundary conditions (i.e. turbulence from last grid cells at outflow boundary are copied to the first grid cell at the inflow boundary) (Bruse & Fleer, 1998: page 375). Temperature and relative humidity at the inflow boundary are forced by the boundary layer model according to a 24 hourly input. The turbulence field is updated every 15 minutes; solar radiation is modelled with a dynamic time step (i.e. smaller when solar radiation is at peak (1 sec) and larger during morning and afternoon (2 sec)); the internal temperature of buildings (free running) is calculated according to the heat transfer through walls and roofs, where all walls and roofs have the same heat transmittance and albedo respectively. The spin-up period was set to 46 hours (starting at 02:00 two days before the simulated day). The main simulation parameters and the input sources are shown in Table 2.

Table 2: Main input parameters for the simulation

Input parameter	August 10, 2013	Source
Specific humidity 2,500 m (750 mbar) *gr w/kg dry air*	13	NCEP/NCAR US (2000)
Prevalent wind direction (N = 0 clockwise)	210	The Weather Underground (2014)
Wind speed 10m ab. gr. *m/s*	2	The Weather Underground (2014)
Roughness length z_0	0.1	Stewart and Oke (2012: page 1890)
Mean wall albedo	0.23	Yang et al. (2013: page 97)
Mean roof albedo	0.50	Yang et al. (2013: page 97)
Wall heat transmittance $W.\ m^{-2}.\ K^{-1}$	1.4	
Roof heat transmittance $W.\ m^{-2}.\ K^{-1}$	0.9	
Underground soil temperature (Upper-Middle-Deep layer) *K*	304	NCEP/NCAR US (2000)
	298	"
	292	"
Underground soil humidity	25 %	NCEP/NCAR US (2000)
(Upper-Middle-Deep layer)	29 %	"
	33 %	"
Timesteps (solar angle < 35 deg)	2 sec	
35 deg. < solar angle< 55 deg	2 sec	
55 deg. < solar angle	1 sec	

The computational domain in ENVI-met comprises an equidistant grid that can be compressed / stretched to the vertical (z, height) dimension by using an expansion ratio but there is no option for the local refinement of the horizontal computational grid. The starting grid cell (i.e. in contact with the ground surface) height was set to 0.5m and the grid remained equidistant below the height of 2.25m with a grid cell spacing equal to dz=0.5m. The combination of a 0.5m starting grid cell height with a 18% grid height expansion ratio resulted in a vertical grid with 16 grid cells at the lower part of the domain (i.e. the lower 20m within the roughness sub-layer). The "urban unit's" 250m radius resulted in 3D computational grids of 72 x 72 x 28 with a resolution of 8m. A sensitivity analysis of the simulation results showed that an increase of the resolution to 6m delivered no significant change in model output.

4. RESULTS AND DISCUSSION

The evaluation of the model's performance showed that urban micro-climate simulations using the newly introduced idealised "urban unit" adequately capture the main characteristics of the diurnal air temperature development (Figure 9). Under a Case 1 set-up, the modelled air temperature at 3.5m above ground ($T_{3.5m}$) peaks at 15:00, an hour earlier than the observed peak in the averaged measured data, but in agreement with some of the sites (background colour lines in Figure 9). However, daytime air temperatures are underestimated with the model failing to predict the maximum temperature. Nevertheless, the simulation results fit well to the observed data at night time, in early morning and afternoon. This could be a result of inaccurate representation of thermal mass and heat storage in the model (Middel et al., 2014: page 21). The prediction of the expected urban heat island during night ($\Delta T_{Case\ -\ NP\ reference}$) is an indication that this level of inaccuracy is not detrimental to the overall function of the model.

In general, the accuracy of the model can be viewed as satisfactory in relation to its purpose, considering the uncertainties involved in the initialisation of the model and the simulation itself. The model performance evaluation indices' scores (Table 3) are similar to other published work (Yang et al., 2013: page 103; Middel et al., 2014: page 20). The index of agreement d takes values in the range {0, 1} with a value of 1 indicating a perfect match between the model prediction and the observations (Willmote, 1982: page 1310; Middel et al., 2014: page 19). The systematic component of the root mean square error (RMSEs) represents the error attributed to the simulation and the error integrated into the initialisation estimates, it should approach 0 (Middel et al., 2014: page 19). The unsystematic component should approach the value of RMSE (Willmote, 1982: page 1311).

Scenario 1 (Cases 1-3) investigated the impact of vegetation's location in relation to the air temperature development ($T_{3.5m}$) at the middle of the idealised urban unit.

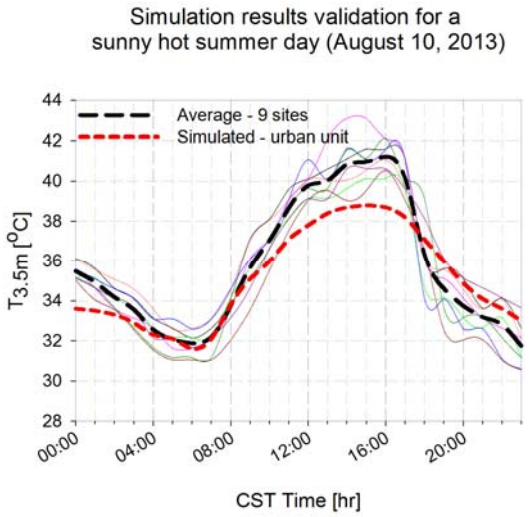

Figure 9: Comparison of the observed and modeled air temperature at 3.5m above ground ($T_{3.5m}$) for August 10, 2013 in Hangzhou. Time in China Standard Time – (CST : GMT+8).

Case 2 that describes the condition where all the vegetation was allocated at the centre of the urban unit returned lower temperatures at the middle grid cell for the largest part of the day (Figure 10, Top). The marginal difference between the cases in Scenario 1 shows that the air temperature development at the middle grid cell captures well the effect of the larger area surrounding it and that it is not only sensitive to the ground surface material of the grid cell itself. Figure 10 depicts the urban heat island intensity at night time and the existence of an urban cool island at day-time that can be attributed to the high aspect ratio (building height to street width ratio) within the urban unit and the high thermal capacity of the built surfaces (Johansson, 2006: page 1332; Erell et al., 2011: page 77). In Scenario 2, the percentage of vegetated surface in the urban unit was increased from 15% in Case 1 to 40% in Case 8 with a step increment of 5% per case. A 40% permeable surface area is the upper limit for the Local Climate Zone 5 classification. The results indicate a very small change in the average $T_{3.5m}$ between the cases, while Case 8 had the lowest temperature for most of the time (Figure 10, Bottom). This is also seen in the frequency of the air temperature occurrences where there is a shift of $T_{3.5m}$ towards lower air temperatures following the increase in vegetated ground surface (Figure 11). High vegetation rates lead to higher frequency of occurrence of lower air temperature values towards the 38 °C end of the histogram. The small change of air temperature in the different vegetated surface ratios is consistent with the Local Climate Zone classification of the sites and it demonstrates the representativeness of the LCZ5 for a distinctive and typical local climate (Stewart et al., 2014: page 11).

In addition, the simulation was run for hot, dry weather that was preceded by 2 days with similar weather conditions. After the spin-up period (46 hrs) the relative soil wetness at 1.5 cm depth was below 10%. It is argued that most of the soil water content evaporated during the spin-up period, significantly

Table 3: Model performance indices

Mean Square Error (MSE): 1.78	index of agreement d: 0.94
Mean Bias Error (MBE): -0.60	Root Mean Square Error (RMSE) : 1.34
MSE systematic: 1.19	MSE unsystematic: 0.58
RMSE systematic: 1.09	RMSE unsystematic: 0.76
Mean Absolute Percentage Error (MAPE): 3.1%	

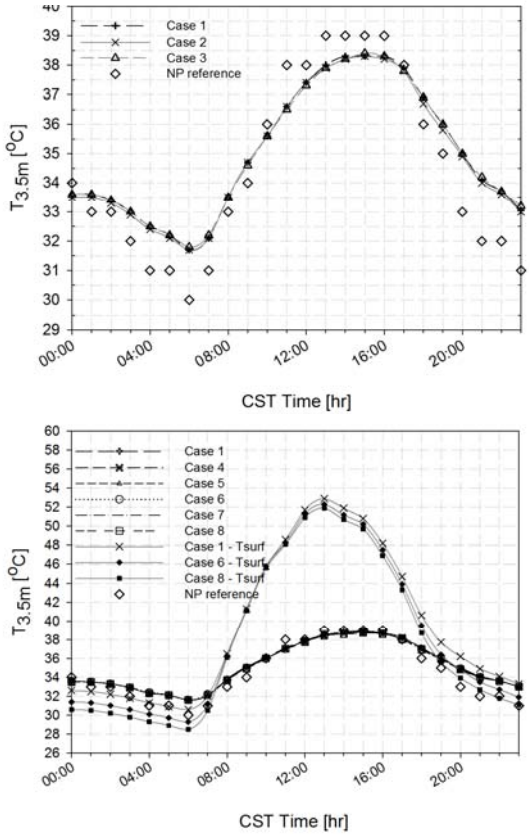

Figure 10: Scenario 1 : Impact of the vegetation's location on the air temperature development ($T_{3.5m}$) at the middle of the "urban unit model" (Top). Scenario 2 : Comparison of the modeled $T_{3.5m}$ and T_{surf} for cases in Scenario 2 (Bottom). Note: NP reference shows the referencemeteorological data from Mantou Mountain weather station.

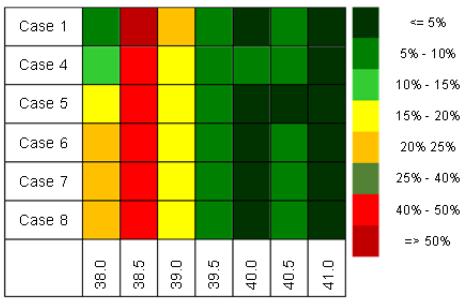

Figure 11: Frequency of occurrence of air temperature (rounded to 0.5 °C) for each Case (1 to 8) in Scenario 2 (rows). Note: Case 2 and 3 are identical to Case 1 in terms of vegetated percentage and not shown. Image adapted from Middel et al., 2014: page 25

reducing the evapotranspiration cooling potential of the vegetation. Lastly, it is to be noted that all the vegetation added in the cases was in the form of grass and the shading effect of vegetation was not taken into account. The impact of vegetation is more evident on the surface temperatures (T_{surf}). The average surface temperature over the urban unit shows a negative correlation with the percentage of permeable ground surface (Figure 10, Bottom). It can also be seen that surface temperatures peak closer in time to the solar noon. The similarity of the surface temperatures during the day-time in the different cases supports the initial argument that evapotranspiration was reduced due to limited water availability. In essence, the absorbed solar radiation led to a surface temperature increase (Erell et al., 2011: page 183) that negated, to a large extent, the effect from any planted surface area added to the urban unit.

5. CONCLUSION

The micro-climate simulations using the newly introduced idealised "urban unit model" showed that the performance of the model was good and that the simulation results displayed a satisfactory accuracy (RMSE: 1.34), comparable to that of previous micro-climate simulation studies (e.g. Yang et al., 2013; Middel et al., 2014). This reveals that there is a potential for the simplification of urban site modelling and for the wider application of the introduced method as a tool for the adaptation of typical meteorological weather data files to the neighbourhood scale urban environment.

The assessment of the impact of the vegetation's location on the air temperature development in the urban canopy revealed that the proximity to "green" – vegetated space can lower the urban heat island intensity during night time and the maximum day-time air temperature. The marginal difference between the cases with a central allocation of the vegetated surface area with those were the vegetation was positioned at the outer border of the urban unit is an indication that the distance to a vegetated area is not enough to alone produce large cooling benefits during the day and attenuate the night time urban heat island intensity. The distance to vegetation must be examined in conjunction with other parameters that can directly affect the urban energy balance, such as the type of vegetation, urban density, wind penetration, soil water content and nearby surface materials' properties. In Scenario 2, an increase to the urban unit's permeable surface area showed a small decrease in the average air temperature across the urban unit. The case with the largest vegetated surface area had the lowest daily air temperatures. A shift was noted in the air temperature distribution towards a higher occurrence frequency of temperatures at the cooler end. The differences between the cases were more evident in the average surface temperatures. The results suggested that high percentages of vegetated space can reduce the surface temperatures within the cities. There were, however, also strong indications that in places with a humid subtropical climate such as Hangzhou, in the case of successive hot, dry summer days, a reduction in soil water content will negate, to a large extent, the cooling benefits of the added vegetation.

6. ACKNOWLEDGEMENTS

The development of the urban unit model and the simulation study is supported and partly funded by the "Liveable Cities Project" (EPSRC funded : EP/J017698/1). The installation work of the sensors' network in Hangzhou and Ningbo is supported by the Ningbo Natural Science Foundation (No. 2012A610173) and the Ningbo Housing and Urban-Rural Development Committee (No. 201206).

7. REFERENCES

Bourikas L., Shen T., James P.a.B., Chow D.H.C., Jentsch M.F., Darkwa J. and Bahaj A.S. (2013) Addressing the challenge of interpreting microclimatic weather data from urban sites *Journal of Power and Energy Engineering,* vol. 1, p.p. 7-15

Bruse M. and Fleer H. (1998) Simulating surface–plant–air interactions inside urban environments with a three dimensional numerical model. *Environmental Modelling & Software,* vol. 13 (3–4), p.p. 373-384

Cheng H. and Castro I.P. (2002) Near wall flow over urban-like roughness. *Boundary-Layer Meteorology,* vol. 104 (2), p.p. 229-259

Crawley D.B. (1998) *Which weather data should you use for energy simulations of commercial buildings? ASHRAE Transactions* 104 Part 2: p.p. 498-515 Atlanta, USA: ASHRAE.

Erell E., Pearlmutter D. and Williamson T. (2011) *Urban microclimate: designing the spaces between buildings.* (1st Edition) London: Earthscan

Hacker J., Capon R. and Mylona A. (2009) Use of climate change scenarios for building simulation: the CIBSE future weather years. London, UK: The Chartered Institution of Building Services Engineers

Johansson E. (2006) Influence of urban geometry on outdoor thermal comfort in a hot dry climate: A study in Fez, Morocco. *Building and Environment,* vol. 41 (10), p.p. 1326-1338

Kanda M. and Moriizumi T. (2009) Momentum and Heat Transfer over Urban-like Surfaces. *Boundary-Layer Meteorology,* vol. 131 (3), p.p. 385-401

Maxim Integrated (2013) *iButton Temperature / Humidity logger with 8 kb data logger memory*. Available from: http://www.maximintegrated.com/products/ibutton/data-logging/

Middel A., Häb K., Brazel A.J., Martin C.A. and Guhathakurta S. (2014) Impact of urban form and design on mid-afternoon microclimate in Phoenix Local Climate Zones. *Landscape and Urban Planning,* vol. 122 (0), p.p. 16-28

Millward-Hopkins J.T., Tomlin A.S., Ma L., Ingham D.B. and Pourkashanian M. (2013) Aerodynamic Parameters of a UK City Derived from Morphological Data. *Boundary-Layer Meteorology,* vol. 146 (3), p.p. 447-468

Mylona A. (2012) The use of UKCP09 to produce weather files for building simulation. *Building Services Engineering Research and Technology*, vol. 33 (1), p.p. 51-62

Ncep/Ncar Us (2000) National Centers for Environmental Prediction (NCEP)/National Weather Service/NOAA/U.S. Department of Commerce. NCEP Final Operational Model Global Tropospheric Analyses, continuing from July 1999. Research Data Archive at the National Center for Atmospheric Research, Computational and Information Systems Laboratory. Boulder CO.,: National Center for Atmospheric Research,

Oke T.R. (2006) Initial guidance to obtain representative meteorological observations at urban sites. *Instruments and observing methods* 2006 (WMO/TD-No. 1250):47 Available from: http://www.wmo.int/pages/prog/www/IMOP/publications/IOM-81/IOM-81-UrbanMetObs.pdf

Santiago J., Martilli A. and Martín F. (2007) CFD simulation of airflow over a regular array of cubes. Part I: Three-dimensional simulation of the flow and validation with wind-tunnel measurements. *Boundary-Layer Meteorology,* vol. 122 (3), p.p. 609-634

Shen T., Chow D.H.C., Cui T. and Darkwa J. (2013) Generating a modified weather data file for urban building design and sustainable urban planning accounting for the Urban Heat Island (UHI) effect. Paper presented at 12th International Conference on Sustainable Energy Technologies. Hong Kong Polytechnic University

Shen T., Chow D.H.C., Darkwa J. and Yao R. (2014) Impact of Urban Heat Island on Building Cooling Energy Consumption in Hangzhou. Paper presented at 13th International Conference on Sustainable Energy Technologies. 25-28 August 2014, Geneva, Switzerland

Stewart I.D. and Oke T.R. (2012) Local Climate Zones for Urban Temperature Studies. *Bulletin of the American Meteorological Society,* vol. 93 (12), p.p. 1879-1900

Stewart I.D., Oke T.R. and Scott Krayenhoff E. (2014) Evaluation of the 'local climate zone' scheme using temperature observations and model simulations. *International Journal of Climatology,* vol. 34, p.p. 1062-1080

The Weather Underground (2014) Hangzhou weather data from Mantou mountain's National Principle WMO-listed weather station

Willmote C.J. (1982) Some comments on the evaluation of model performance. *Bulletin of the American Meteorological Society,* vol. 63 (11), p.p. 1309-1313

Xie Z. and Castro I.P. (2006) Large-eddy simulation for urban micro-meteorology. *Journal of Hydrodynamics, Ser. B,* vol. 18 (3, Supplement), p.p. 259-264

Yang X., Zhao L., Bruse M. and Meng Q. (2013) Evaluation of a microclimate model for predicting the thermal behavior of different ground surfaces. *Building and Environment,* vol. 60, p.p. 93-104